# $^{23}Na$, $^{27}Al$ and $^{31}P$ NMR and X-ray powder diffraction study of Na/Ca/Al phosphate glasses and ceramics

**Isaac Abrahams,[a] Katrin Franks,[a] Geoffrey E. Hawkes,*[a] George Philippou,[a] Jonathan Knowles,[b] Philippe Bodart[c]† and Teresa Nunes[c]**

[a]*Structural Chemistry Group, Department of Chemistry, Queen Mary & Westfield College, University of London, Mile End Road, London, UK E1 4NS*

[b]*Eastman Dental Institute, University of London, 256 Gray's Inn Road, London, UK WC1X 8LD*

[c]*ICTPOL, Av. Prof. Gama Pinto 2, 1699 Lisboa codex, Portugal*

The techniques of X-ray powder diffraction and solid-state magic angle spinning (MAS) $^{23}Na$, $^{27}Al$, and $^{31}P$ nuclear magnetic resonance (NMR) spectroscopy have been combined to investigate the speciation in a series of glasses and glass ceramics of general formula $(P_2O_5)_{0.45}(CaO)_{0.24}(Na_2O)_{0.31-x}(Al_2O_3)_x$, $x=0.0$–$0.05$. The principal phosphate species are shown to be various $P_2O_7^{4-}$ containing phases, and cylic trimetaphosphates bridged by Ca, *i.e.* $Na_4Ca(PO_3)_6$ (instead of open-chain metaphosphates). Higher concentrations of $Al_2O_3$ result in glass ceramics which are phosphate-depolymerised ($Q^2 \rightarrow Q^1$) with respect to the parent glasses. At a lower level of $Al_2O_3$ (2%) the aluminium is present in octahedral coordination, while the higher level (5%) results in the formation of tetrahedrally coordinated aluminium. X-Ray powder diffraction of the ceramic with the higher aluminium content indicated the presence of $Na_5Ca_2Al(PO_4)_4$, and the $^{31}P$ NMR spectrum provides evidence for $Q_1^2$ species similar to phosphorus in aluminium metaphosphate. The more detailed structural information available from the aluminium-free glass ceramic, and the similarity in the $Q^1/Q^2$ ratio between the glass and its derived ceramic leads to the thesis that the ceramic structure may, in favourable cases, be used to model phosphate speciation in the glass.

There is a general need for some type of bone replacement for patients who have suffered from trauma, chronic degenerative diseases leading to bone loss, or congenital abnormalities. Some bioactive materials are available, which might potentially be used in this clinical situation and they are based on calcium phosphates,[1] *e.g.* hydroxyapatite (HA), tricalcium phosphate (TCP), fluorapatite (FHA). The bioactivity of these materials is normally attributed to their close chemical relationship to the inorganic phase of bone. Other bioactive materials are also available based on silicates, *e.g.* Bioglass®, and apatite wollastonite glass ceramic (AWGC),[2] which maintain high bioactivity through a dissolution–reprecipitation mechanism as opposed to a close chemical affinity. These materials however, have serious limitations. Firstly, the calcium phosphate based materials are crystalline compounds and their chemistry may not easily be altered, due to their stoichiometry. The second group of materials are hindered in their use by being silicate based and are therefore essentially insoluble and furthermore, their long-term effects are unknown. In this respect soluble phosphate glasses and glass ceramics offer potential advantages, particularly the ability to alter the solubility to a rate suitable for the application. The development of bioactive glass ceramics has been reviewed by Vogel and Höland.[3] Our interest focuses on $CaO$–$Na_2O$–$P_2O_5$ glasses including structure-modifying oxides, and we present here our data on these glasses doped with $Al_2O_3$.

In order to optimise the glasses, techniques need to be applied to probe their chemistry and currently, because of the non-crystalline nature of glasses, the number of techniques available is few. Solid-state nuclear magnetic resonance (NMR) is one of these few techniques and it can give a wealth of information, which may be used to develop models relating the chemical structure and bonding to the bioactivity of the glass. The application of NMR to the study of phosphate glasses has been recently reviewed by Kirkpatrick and Brow.[4]

† Present address: Department of Chemistry, University of Durham, South Road, Durham, UK DH1 3LE.

$^{31}P$ NMR spectroscopy is particularly useful and can enable the quantification of the relative amounts of $Q^n$ phosphorus species present, $\boldsymbol{P}O_{4-n}(OP)_n$, since in favourable cases resonances due to each of these species are resolved in the magic angle spinning (MAS) spectra. Hartmann *et al.*[5] used $^{31}P$ NMR in their study on a series of Ca/Na/Al/phosphate glasses and ceramics and found predominantly $Q^1$ and $Q^2$ phosphorus units. Their aluminium-free glasses contained 39–53% $Q^2$ units, and for glasses containing aluminium they found a significant decrease in $Q^2$ content from 67 to 30% as the $Al_2O_3$ content increased from 1.1 to 3.1%. In a subsequent investigation on glasses and ceramics of similar composition Hartmann *et al.*[6] used $^{31}P$ 2D exchange NMR to show the contribution of pyrophosphate to the $Q^1$ region of the spectrum, and also showed a connectivity between the $Q^1$ and $Q^2$ regions indicating the presence of open chain metaphosphate groups. Fletcher *et al.*[7] reported qualitative $^{31}P$ NMR data on binary calcium phosphate glasses which showed $Q^1$, $Q^2$ and $Q^3$ units. Brow *et al.*[8] quantified $Q^1$, $Q^2$ and $Q^3$ units from binary sodium phosphate glasses, whereas Born and coworkers[9,10] found only $Q^2$ and $Q^3$ units in a sodium phosphate glass and from $^{31}P$ 2D NMR experiments showed connectivity between the two types of unit suggesting an almost regular alternating sequence for the $Q^2$ and $Q^2$ units.

For glasses incorporating $Al_2O_3$, $^{27}Al$ MAS NMR spectra can be used[4] to quantify relative amounts of four-, five-, or six-coordinate aluminium in the structure. $^{23}Na$ MAS NMR has been applied in relatively few studies[8,11] of glasses, and the information content from these spectra has been restricted by their relatively poor resolution and the relatively large second-order quadrupole effects which influence the spectra. More recently Koller *et al.*[12] presented a systematic analysis of the $^{23}Na$ NMR parameters from a series of crystalline sodium compounds, and their data may provide a sound basis for the interpretation of spectra from glasses.

Heating of glasses above the glass transition temperature $T_g$ results in crystallisation within the glass matrix to form a glass ceramic. The phases crystallised in this way can be stoichio-

metric or non-stoichiometric depending on the parent glass. Materials prepared in this way generally contain a mixture of crystalline phases with some residual glass. Whilst the individual phases may not reflect the composition of the original glass the overall composition is the same. The advantage of crystallising glasses is that other techniques such as X-ray powder diffraction can then be used in the study of the material and the results extrapolated to the glass. In addition the NMR linewidths of crystalline phases are much narrower due to the smaller range of chemical environments in ordered crystalline solids when compared to glasses.

We present here our $^{23}$Na, $^{27}$Al and $^{31}$P MAS NMR and X-ray powder diffraction data on a series of glasses and glass ceramics of general formula $(P_2O_5)_{0.45}(CaO)_{0.24}(Na_2O)_{0.31-x}(Al_2O_3)_x$, $x=0.0$–$0.05$. This composition was chosen because it has an accessible melting point, and glasses with this composition are likely to exhibit a significant bioactivity.[3] The Ca/P ratio was held constant in order to minimise the number of variables across the quaternary glass series.

## Experimental

### Preparation of glasses and ceramics

Samples of three glass compositions were prepared using appropriate molar quantities of $CaCO_3$, $NaH_2PO_4$, $CaHPO_4$, $P_2O_5$ and $AlPO_4$. The mixtures were blended in a Seward 400 stomacher prior to heating, and were then melted at 1200 °C in a platinum crucible for 1 h. Previous work[8,13] has shown that compositional changes due to evaporation of volatile components during glass formation in such materials are negligible especially over short intervals as used in this study. The melt was then poured into a preheated (600 °C) graphite mould and slowly cooled from 600 °C to room temperature at 4 °C min$^{-1}$. The glass rods produced of approximately 12 mm diameter were cut into discs of approximately 2 mm thickness using a diamond saw.

Investigation of crystallisation and glass transition temperatures was carried out by differential scanning calorimetry using a Perkin Elmer DSC 7, varying the temperature from 25 to 600 °C at a heating rate of 20 °C min$^{-1}$. Subsequent conversion to ceramic samples was carried out by heating glass discs on gold foil for *ca.* 2–3 h at temperatures just below the crystallisation temperatures. The compositions of the glasses and conditions for crystallisation are summarised in Table 1.

### X-Ray crystallography

X-Ray diffraction data were collected on powdered glass ceramic samples on a Siemens D5000 diffractometer in flat-plate mode using graphite-monochromated Cu-K$\alpha$ radiation ($\lambda=1.5418$ Å). Data were collected in the range $2\theta$ 10–90°, in steps of 0.03°. Data for glass ceramic **3** were collected on an automated Philips PW 1280 diffractometer in flat-plate mode using nickel-filtered Cu-K$\alpha$ radiation in the range $2\theta$ 5–70°, in steps of 0.02°.

**Table 1** Compositions (%) of the glasses and crystallisation conditions

| | glass **1** | glass **2** | glass **3** |
|---|---|---|---|
| $P_2O_5$ | 45 | 45 | 45 |
| $Na_2O$ | 31 | 29 | 26 |
| CaO | 24 | 24 | 24 |
| $Al_2O_3$ | 0 | 2 | 5 |
| $T_g$[a]/°C | 250 | 380 | 415 |
| $T_c$[b]/°C | 478 | 522 | — |
| ceram.[c] | 2 h, 430 °C | 2 h, 520 °C | 3 h, 539 °C |

[a]The glass transition temperature. [b]The crystallisation temperature. [c]The length of time and temperature (°C) for ceramic formation.

### NMR spectroscopy

The one-dimensional single-pulse $^{23}$Na, $^{27}$Al and $^{31}$P spectra were measured in London using a Bruker MSL-300 spectrometer operating at 79.4 MHz for $^{23}$Na, 78.2 MHz for $^{27}$Al and 121.5 MHz for $^{31}$P. The samples were contained in 4 mm o.d. rotors and magic angle spinning (MAS) was used at *ca.* 10–11 kHz for $^{23}$Na and $^{27}$Al, and 7.5 kHz for $^{31}$P. Typically 300–1000 transients were acquired for the $^{23}$Na spectra using a 2 s relaxation delay, up to 10 000 transients for the $^{27}$Al spectra with a 0.5 s relaxation delay, and 16 transients for the $^{31}$P spectra using a 60 s relaxation delay. The two-dimensional triple-quantum MAS spectrum[14–16] was measured in Lisbon using a Bruker MSL-300 spectrometer. The sample was contained in a 4 mm o.d. rotor and MAS used at 14 kHz; 72 transients were acquired with a 10 s recycling time; 512 and 256 points were acquired in the F1 and F2 dimensions respectively.

### NMR spectral simulation

The $^{23}$Na MAS NMR spectra were simulated using the program QUASAR.[17] The overlapping resonances in the $^{31}$P MAS NMR spectra were deconvoluted using the XEDPLOT routine within the Bruker XWINNMR software.

## Results

### $^{23}$Na solid-state NMR spectra

The single-pulse solid-state magic angle spinning (MAS) $^{23}$Na NMR spectra of the glass **1** and the corresponding ceramic are shown in Fig. 1. The overall widths of the two spectra are about the same, however it is clear that there is significantly improved resolution of the band shape for the ceramic. It appeared likely that there were two chemical shifts contributing to the spectrum of the ceramic, and to confirm this the two-dimensional triple quantum MAS spectrum[14–16] was acquired.

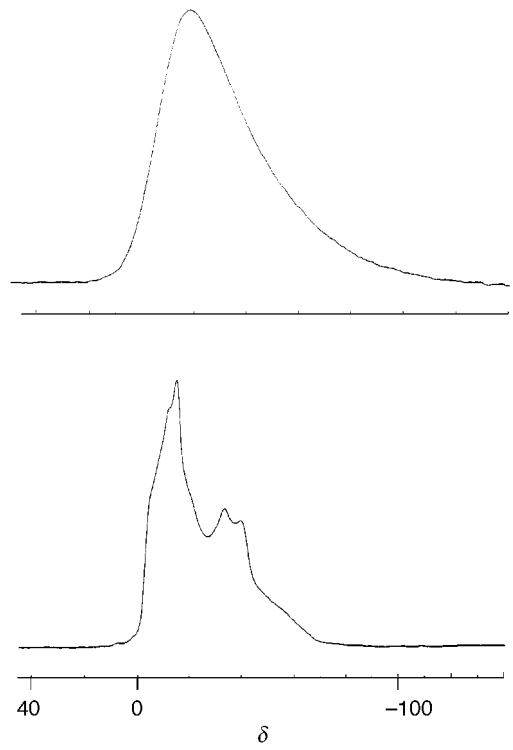


**Fig. 1** The 79.4 MHz $^{23}$Na MAS NMR spectra of glass **1** (upper) and ceramic **1** (lower). For both spectra the MAS rate was 10.5 kHz.

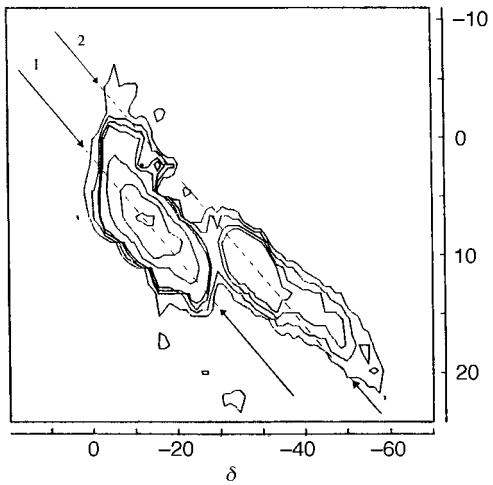


**Fig. 2** The 79.4 MHz $^{23}$Na triple quantum 2D MAS NMR spectrum of ceramic **1**. The MAS rate was 14 kHz and the diagonal arrows indicate the two distinct sites.

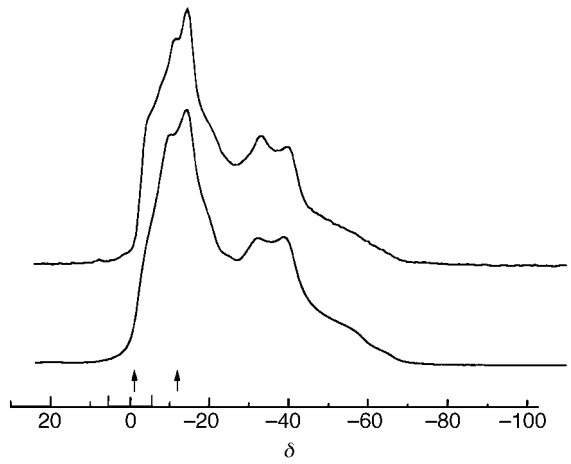


**Fig. 3** Experimental (upper) and simulated (lower) 79.4 MHz $^{23}$Na MAS NMR spectrum of ceramic **1**. The parameters from the simulation are given in Table 2, and the arrows indicate the isotropic chemical shifts.

The result is shown in Fig. 2, which shows two principal sodium sites. The extractable parameters from the spectrum are the isotropic chemical shifts and the 'second order quadrupole' parameters[15] (SOQE):

$$\mathrm{SOQE} = C_\mathrm{q}\left(1+\frac{{\eta_\mathrm{q}}^2}{3}\right)^{1/2} \quad (1)$$

where $C_\mathrm{q}$ and $\eta_\mathrm{q}$ are the quadrupole coupling constant and asymmetry parameter respectively, and the values obtained are given in Table 2.

With the information from the 2D-3Q MAS experiment as a starting point the single-pulse $^{23}$Na MAS spectrum was simulated. The parameters obtained from this fitting procedure are also collected in Table 2, and the calculated spectrum is shown in Fig. 3. As can be seen there is good agreement between the quadrupole coupling parameters from the two methods, and between the isotropic shifts. There is a small difference (2–3 ppm) in the isotropic shifts from the two experiments, and those values from the single-pulse spectrum are probably the more reliable. The $^{23}$Na spectrum of ceramic **3** was similarly fitted as two sodium sites (Table 2) while that for ceramic **2** showed evidence, at the high-frequency edge of the band, for a third site. The spectrum of ceramic **2** was fitted as three sites (Fig. 4) and gave the parameters in Table 2.

### $^{27}$Al solid-state NMR spectra

The $^{27}$Al data for the glasses and ceramics **2** and **3** are given in Table 3. The chemical shifts are measured directly from the spectra and so are not corrected for the quadrupolar shift.

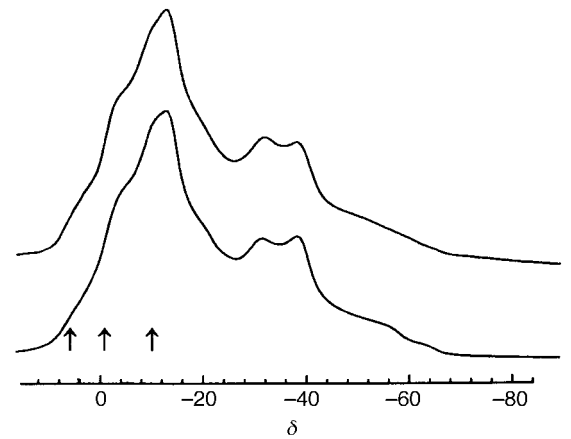


**Fig. 4** Experimental (upper) and simulated (lower) 79.4 MHz $^{23}$Na MAS NMR spectrum of ceramic **2**. The parameters from the simulation are given in Table 2, and the arrows indicate the isotropic chemical shifts.

### $^{31}$P solid-state NMR spectra

The solid-state $^{31}$P MAS spectra of glass **1** and of ceramic **1** are shown in Fig. 5. As with the $^{23}$Na spectra (Fig. 1) the spectra are basically similar, but that of the ceramic shows considerably improved resolution, and it is possible to resolve eight resonances in the high-frequency band (band B, $\delta$ 0 to $-10$) and four resonances in the low-frequency band (band A, $\delta$ $-20$ to $-23$). The integrated intensities of the individual lines were determined by deconvolution of the experimental

**Table 2** $^{23}$Na NMR parameters for the ceramics

| | $\delta_{iso}$[a] | site occupancy (%) | SOQE/MHz | $C_q$/MHz | $\eta_q$ |
|---|---|---|---|---|---|
| ceramic **1** | −2.7 | | 1.59 | | |
| (2D-3Q) | −13.4 | | 2.47 | | |
| ceramic **1** | −0.7 | 45±2 | 1.62 | 1.55±0.03 | 0.53±0.05 |
| (single pulse) | −10.3 | 55±2 | 2.45 | 2.27±0.04 | 0.69±0.05 |
| ceramic **2** | −2.4 | 40±2 | | 1.52±0.01 | 0.68±0.01 |
| (single pulse) | −11.4 | 48±2 | | 2.26±0.01 | 0.72±0.01 |
| | 5.7 | 12±2 | | 1.41±0.04 | 0.50±0.1 |
| ceramic **3** | −1.8 | 44±2 | | 1.51±0.01 | 0.60±0.01 |
| (single pulse) | −10.6 | 56±2 | | 2.36±0.02 | 0.65±0.02 |

[a]The chemical shifts are referenced to external NaCl solution. We are unable to estimate the error on the shifts from the 3Q MAS experiment, but the errors are ±0.4 and ±0.8 ppm respectively for the high- and low-frequency signals from the single-pulse experiment.

**Table 3** $^{27}$Al NMR data for the glasses and ceramics

| | $\delta^a$ | $\Delta\nu_{1/2}{}^b$/Hz |
|---|---|---|
| glass **2** | −15<br>(10, 37)[c] | 540<br>(*ca.* 500)[c] |
| ceramic **2** | −14, −21 | 130 |
| glass **3** | −16<br>(8, 33)[c] | 620<br>(*ca.* 500)[c] |
| ceramic **3** | −17 (93%)<br>39 (7%) | 220<br>150 |

[a]Chemical shifts in ppm to high frequency of external 1.0 M $AlCl_3$. [b]Full-width at half height. [c]These are minor resonances that constitute <10% of the total $^{27}$Al spectrum.

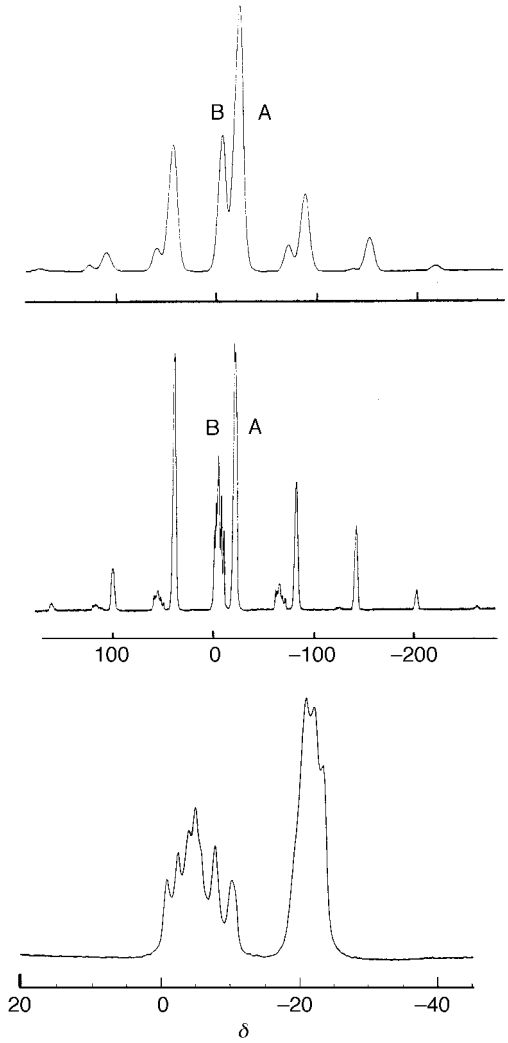


**Fig. 5** The 121.5 MHz $^{31}$P MAS NMR spectra of: (upper) glass **1** with MAS rate 8.0 kHz, (middle) ceramic **1** with MAS rate 7.4 kHz, (lower) expansion of the centre band region for ceramic **1**

spectrum, as described in the Experimental section, and the total intensity of each band (A and B) was obtained by summation over all spinning side-bands. The result for glass **1** was band B 22% and band A 78%, and for ceramic **1** band B 29% and band A 71%. A similar analysis was performed for glasses and ceramics **2** and **3**, and the results are given in Table 4. For ceramic **2** bands A and B were treated as comprising four and eleven overlapping resonances respectively, and for ceramic **3** these two bands comprised four and ten overlapping resonances. In addition the spectrum of ceramic **3** showed two new bands C (a single resonance) and D (three overlapping resonances). The results of deconvolution of bands B and A are shown schematically in Fig. 6 and 7 respectively. For the ceramic samples the isotropic chemical shift ($\delta_{iso}$, Table 4) for each band is calculated by:

$$\delta_{iso} = \sum_i n_i \delta_i \quad (2)$$

where the index $i$ runs over the number of resonances within that band, $\delta_i$ is the shift of each resonance and $n_i$ is the fractional intensity of the $i$th resonance in that band. The full width at half height ($\Delta\nu_{1/2}$) quoted in Table 4 for each band is the average for the resolved resonances in that band.

The intensities of the spinning side bands were analysed by the method of Herzfeld and Berger,[18] as we have previously described.[19] This analysis yields the principal components ($\delta_{11}$, $\delta_{22}$, $\delta_{33}$) of the chemical shift tensor, for which the isotropic chemical shift ($\delta_{iso}$) is given by:

$$\delta_{iso} = (\delta_{11} + \delta_{22} + \delta_{33})/3 \quad (3)$$

These principal elements were ordered according to the Haeberlen convention:[20] $|\delta_{33} - \delta_{iso}| > |\delta_{11} - \delta_{iso}| > |\delta_{22} - \delta_{iso}|$. The chemical shift anisotropy ($\Delta\delta$) and asymmetry parameter ($\eta$) are given by:

$$\Delta\delta = \delta_{33} - (\delta_{11} + \delta_{22})/2 \quad (4)$$

$$\eta = (\delta_{22} - \delta_{11})/(\delta_{33} - \delta_{iso}) \quad (5)$$

These data are reported in Table 4 for each of the bands in the glasses and the ceramics. The analysis was not performed for the individual resonances within band A and within band B because of the large errors in the integrals of these resonances in the weaker side bands.

A selected range of the X-ray patterns for the three glass ceramic samples are shown in Fig. 8. The pattern for ceramic **1** has been successfully indexed[21] with $Na_4Ca(PO_3)_6$ as the major phase. Ceramic **2** has a similar pattern and again indicates that $Na_4Ca(PO_3)_6$ is the major phase present with a slight shift in lattice parameters, indicative of solid-solution formation with aluminium. At 5% $Al_2O_3$ in ceramic **3** the appearance of a second major phase, which has been indexed as $Na_5Ca_2Al(PO_4)_4$ based on the reported crystal structure,[22] suggests that this phase becomes increasingly more favoured as the Al concentration increases. Again a shift in lattice parameters for $Na_4Ca(PO_3)_6$ is observed. Table 5 summarises the $Na_4Ca(PO_3)_6$ lattice parameter variation with ceramic composition.

## Discussion

### $^{23}$Na solid-state NMR spectra

Inspection of the data in Table 2, from the fitting of the single-pulse spectra, shows two principal sodium sites with isotropic chemical shifts $\delta$ $-1.6 \pm 0.9$ and $-10.7 \pm 0.6$, and the occupancy of the lower frequency site is slightly greater. The quadrupole coupling constants are consistent over the three ceramics with values 1.4–1.6 MHz and 2.3–2.4 MHz, respectively for the low- and high-frequency sites. There is a paucity of published $^{23}$Na solid-state NMR data on sodium phosphate phases, but it is noteworthy that the parameters obtained here are very similar to those measured by Koller *et al.*[12] for the cyclic trimetaphosphate phase $Na_3P_3O_9$, wherein there are[23] two equally populated, five-coordinate sodium sites.

### $^{27}$Al solid-state NMR spectra

The features of the aluminium spectra reported in Table 3 have also been measured by Hartmann *et al.*[5] The lower frequency resonances in the range $\delta$ −14 to −21 are due to aluminium octahedrally coordinated by oxygens, $Al(OP)_6$ (see Brow *et al.*[24]), while the higher frequency band ($\delta$ 33–39) is most likely[25] arising from four-coordinate aluminium, probably as $AlPO_4$. The signals at intermediate chemical shift, $\delta$ 8–10, are

**Table 4** $^{31}$P chemical shift[a] tensor components for the glasses and the ceramics

| | %[b] | $\delta_{iso}$ | $\Delta\nu_{1/2}$[c] | $\delta_{11}$ | $\delta_{22}$ | $\delta_{33}$ | $\Delta\delta$ | $\eta$ |
|---|---|---|---|---|---|---|---|---|
| glass **1** | | | | | | | | |
| band B ($Q^1$) | 22 | −5 | 940 | −80 | −22 | 87 | 138 | $0.6_2$ |
| band A ($Q^2$) | 78 | −21 | 1190 | 77 | 16 | −158 | −204 | $0.4_5$ |
| ceramic **1** | | | | | | | | |
| band B ($Q^1$) | 29 | −5.1 | 137 | −73 | −21 | 80 | 127 | $0.6_1$ |
| band A ($Q^2$) | 71 | −21.1 | 183 | 91 | 25 | −181 | −239 | $0.4_2$ |
| glass **2** | | | | | | | | |
| band B ($Q^1$) | 27 | −7 | 1360 | −88 | −15 | 82 | 134 | $0.8_1$ |
| band A ($Q^2$) | 73 | −21 | 1430 | 73 | 13 | −149 | −192 | $0.4_7$ |
| ceramic **2** | | | | | | | | |
| band B ($Q^1$) | 49 | −10.6 | 199 | −87 | −20 | 75 | 128 | $0.7_8$ |
| band A ($Q^2$) | 51 | −21.1 | 175 | 91 | 26 | −179 | −238 | $0.4_1$ |
| glass **3** | | | | | | | | |
| band B ($Q^1$) | 25 | −9 | 1313 | −86 | −27 | 87 | 143 | $0.6_1$ |
| band A ($Q^2$) | 75 | −21 | 1729 | 63 | 11 | −138 | −175 | $0.4_4$ |
| ceramic **3** | | | | | | | | |
| band C ($Q^1$) | 4 | −0.4 | 1035 | −86 | −9 | 94 | 141 | $0.8_3$ |
| band B ($Q^1$) | 41 | −10.0 | 204 | −87 | −16 | 73 | 124 | $0.8_6$ |
| band A ($Q^2$) | 44 | −20.5 | 202 | 74 | 25 | −159 | −209 | $0.3_5$ |
| band D ($Q_1^2$) | 11 | −28.3 | 187 | −91 | −35 | 41 | 104 | $0.8_1$ |

[a] $^{31}$P chemical shifts, $\delta_{iso}$, the tensor components $\delta_{ii}$, and the anisotropy, $\Delta\delta$, are in ppm. The chemical shifts are referenced to external 85% aqueous phosphoric acid. Errors on the $\delta_{ii}$ values estimated to be *ca.* ±5 ppm for the ceramic bands $Q^1$ and $Q^2$ the isotropic chemical shifts are the weighted average of the shifts of the individual resonances within the band. [b] Errors are believed to be <10% of the stated value. [c] Full width at half height of the resonances, obtained from deconvolution of the MAS spectra as described in the Experimental section. For the ceramics the values given are the average of the individual resonances within that band. Errors are *ca.* ±90 Hz for the glasses.

**Table 5** Variation of lattice parameters for $Na_4Ca(PO_3)_6$ with ceramic composition

| ceramic | $a$/Å | $b$/Å | $c$/Å | $\beta$/° | $V$/Å$^3$ |
|---|---|---|---|---|---|
| **1** | 13.06(13) | 8.04(8) | 14.46(12) | 94.1(3) | 1515 |
| **2** | 13.11(9) | 8.05(5) | 14.32(8) | 94.7(2) | 1506 |
| **3** | 13.18(8) | 7.90(17) | 14.03(9) | 94.2(4) | 1456 |

more difficult to assign unambiguously. Dupree *et al.*[26] reported octahedral $Al(OAl)_6$ shifts in the range $\delta$ 1–12, while Brow *et al.*[24] assign a $^{27}$Al peak at $\delta$ 15, from a sodium aluminophosphate glass to arise from five-coordinate $Al(OP)_5$ sites. Hartmann *et al.*[5] assigned $^{27}$Al peaks at $\delta$ *ca.* 11, from Na/Ca/Al/phosphate glasses to $Al(OM)_6$ (M = metal) sites. The linewidths of the intermediate shift $^{27}$Al peaks in this study are *ca.* 6 ppm, and therefore we are probably observing signals from the six-coordinate Al sites with metal in the second coordination sphere, but we cannot categorically exclude the five-coordinate Al sites.

### $^{31}$P solid-state NMR spectra

The spectra of both the glasses and the ceramics consist of two principal bands each, with the lower frequency band A assigned to $Q^2$ phosphate units and band B to $Q^1$ units (see Table 4). The assignment of these bands respectively to $Q^1$ and $Q^2$ phosphate units has recently been discussed by Hartmann *et al.*[5] The isotropic chemical shifts fall within the ranges quoted by Haubenreisser *et al.*[27] for polycrystalline phosphates as $\delta$ 4 to −33 for $Q^1$ units and $\delta$ −18 to −53 for $Q^2$ units. In addition the $^{31}$P chemical shift anisotropies for the $Q^1$ and $Q^2$ units were originally established[27] to be in the ranges $\Delta\delta$ 14–80 and −160 to −250 respectively. Our values for band B in the glass and ceramic ($\Delta\delta$ 138 and 127) are outside that original range, but in agreement with the subsequent data of Hartmann *et al.*[5] for $Q^1$ units with sodium and calcium ions in the second coordination sphere ($\Delta\delta$ = 137 ± 6). The values for $\Delta\delta$ reported here for band A in the glass and the ceramic ($\Delta\delta$ −204 and −239) are within the range quoted by Haubenreisser *et al.*[27] (see above) and similar to the values ($\Delta\delta$ −176 and −204) for the Ca/Na/Al/phosphate glasses and ceramics studied by Hartmann *et al.*[5]

The individual chemical shift tensor components determined here for band B (Table 4) in both the glass and ceramic are close to the values indicated by Haubenreisser *et al.*[27] for $Q^1$ units ($\delta_{ii}$ −55, −30 and +75), and similarly the values here for band A are close to the reported values for $Q^2$ units ($\delta_{ii}$ +80, +20 and −155).

When Hartmann *et al.*[5] formed ceramics from their glasses they obtained incomplete crystallisation, but in their ceramic phases there was a clear reduction in the $Q^2$ content for those samples containing $Al_2O_3$, whereas they reported no such reduction for the aluminium-free samples. Our ceramic **1** contains no detectable glass contamination, is aluminium free, but does show a slight reduction (*ca.* 7%) in $Q^2$ content when compared with the glass. However this reduction is not significantly greater than the error limits (*ca.* ±5%) we estimate from the integrations.

### Composition of the glasses

A major difference between the data reported here and that of the glasses prepared by Hartmann *et al.*[5] is the relative proportion of the $Q^1$ and $Q^2$ units. The aluminium-free $CaO/Na_2O/P_2O_5$ glasses from Hartmann *et al.*[5] contained 39–53% of $Q^2$ units, and those glasses with low levels of $Al_2O_3$ contained 67–30% $Q^2$ units. For all three glasses in this study the $Q^2$ content is in the range 73–78% and clearly the presence of aluminium in our glass structures, at the expense of sodium, does not significantly change the $Q^1/Q^2$ ratio. This observation is in contrast to that of Hartmann *et al.*[5] who observed a significant decrease in $Q^2$ content with increase in $Al_2O_3$. However in those glasses investigated by Hartmann *et al.*[5] other factors varied, for example they maintained a fairly constant mol% $Na_2O$ (*ca.* 28.4%) whereas the atom ratio P/Ca varied in the range 2.17–2.69. In the glasses reported here the atom ratio P/Ca was constant at 3.75 and the mol% $Na_2O$ varied in the range 26–31%. The preponderance of $Q^2$ units over $Q^1$ units in our samples suggests a relatively high proportion of cyclic phosphate structures.

To consider the effect of aluminium content on the glass

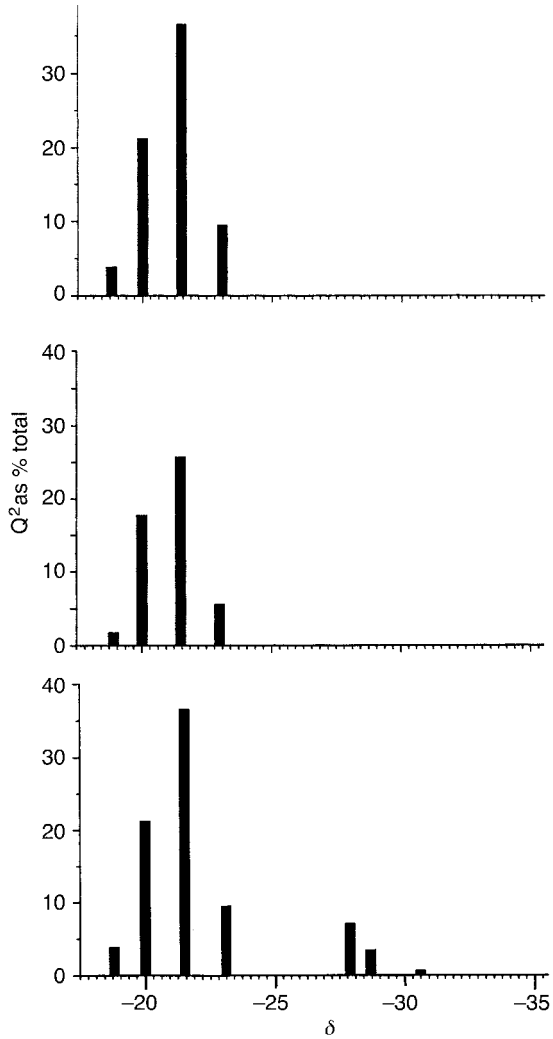


**Fig. 6** Schematic presentation of the results of deconvolution of the $^{31}P$ resonance bands A for the ceramics **1** (upper), **2** (middle), and **3** (lower). The height of the bars indicates the total integrated intensity of each resonance and does not reflect the width of the resonance.

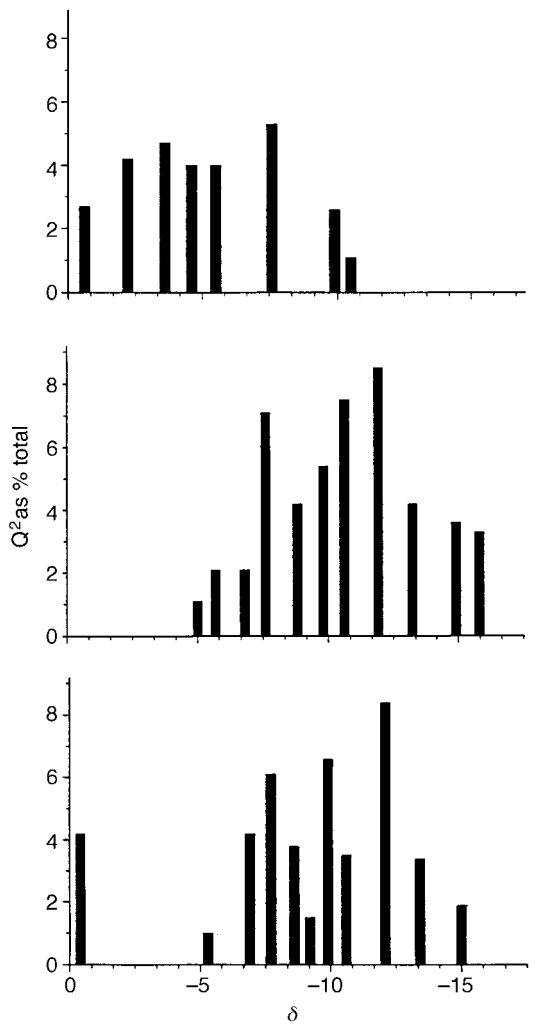


**Fig. 7** Schematic presentation of the results of deconvolution of the $^{31}P$ resonance bands B for the ceramics **1** (upper), **2** (middle), and **3** (lower); this also includes band C at $\delta$ −0.7. The height of the bars indicates the total integrated intensity of each resonance and does not reflect the width of the resonance.

structure we note that the glass transition temperature ($T_g$) increases with increase in the aluminium content (Table 1). This observation is in agreement with that of Brow *et al.*[24,28] who ascribed the effect in sodium aluminophosphate glasses as being due to $Al(OP)_6$ species altering and strengthening the glass network by cross-linking neighbouring phosphate chains. The data in Table 4 for the glasses show that increasing aluminium content results in a slight low-frequency shift for the $Q^1$ signal without significantly affecting the position of the $Q^2$ signal. By comparison with the model studies on $^{31}P$ shifts from crystalline ortho-,[29–31] pyro-[30,31] and meta-phosphates[31] such low-frequency shifts would be expected from replacement of P—O$^-$Na$^+$ or P—O$^-$Ca$^{2+}$ by P—O—Al bonds in the structure. We use the 'Q' nomenclature for aluminophosphate species as suggested by Grimmer and Wolf;[32] *i.e.* $Q_m^n$ where as before $n$ is the number of coordinated —OP groups and $m$ is the number of coordinated —OAl groups. Therefore the low-frequency shift is due to the change $Q_0^1 \rightarrow Q_1^1$ (in agreement with the observations of Brow *et al.*[24]). The effect of the low levels of aluminium on the linewidths of the $Q^1$ and $Q^2$ resonances is that for 0–2% $Al_2O_3$ (glass **1** to glass **2**) there is an approximately 45% increase in the width of the $Q^1$ resonance, while the width of the $Q^2$ resonance increases by 20%. Such increases in the linewidth can arise from a greater diversity of the metal ions in the second coordination sphere of phosphorus (see above) and a greater spread in P—O—P and O—P—O bond angles.[33] Further increase in the level of $Al_2O_3$ from 2 to 5% (glass **2** to glass **3**) does not result in an increase of the width of the $Q^1$ resonance. There is however a further 21% increase in the width of the $Q^2$ resonance which may be due to the bond angle effect or to the inclusion of lower-frequency, aluminium-containing components (see below the discussion of band D in ceramic **3**).

### Composition of the ceramics

A comparison of the schematic $^{31}P$ spectra (Fig. 6) shows band A in all three ceramics is dominated by the same four isotropic chemical shifts ($\delta$ −18.9, −19.9, −21.5 and −23.0), which have approximately the same relative intensities within each spectrum. These four resonances contribute somewhat less to the total $^{31}P$ spectrum for ceramic **2** than for ceramics **1** and **3**. These isotropic chemical shifts are characteristic of metaphosphate groups ($Q^2$) with sodium ions in the second coordination sphere of phosphorus; for example, Prabhakar *et al.*[31] reported five resolved resonances in the region $\delta$ −15.6 to −26.8 from crystalline $(NaPO_3)_n$, and commented that the number of resonances was not simply related to (being greater than) the number of crystallographically distinguishable phosphorus sites. It is likely that the four component signals of band A observed in this study, which have quite different relative intensities, are due to a mixture of phases. This is consistent with the X-ray data. The predominance of $Q^2$ units is indicative of cyclic or long-chain phosphates. The crystal

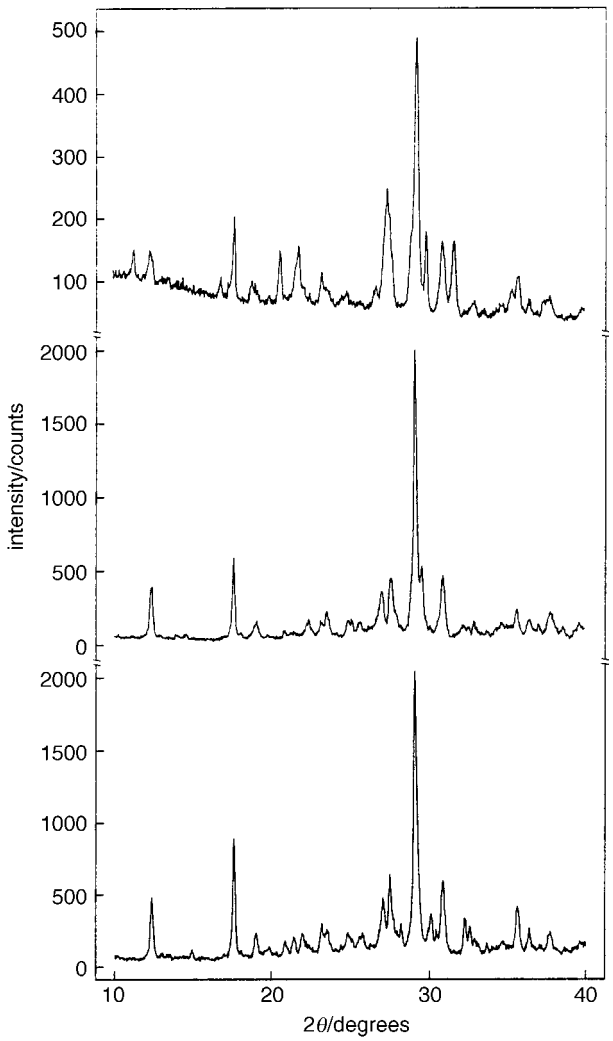


**Fig. 8** X-Ray powder diffraction patterns in the range $2\theta = 10$–$40^\circ$ for ceramics **1** (lower), **2** (middle), and **3** (upper)

structure of the major phase present, $Na_4Ca(PO_3)_6$, is unknown, however it has been suggested[34] that the structure is a calcium-bridged trimetaphosphate (Fig. 9). The change in $Q^1/Q^2$ ratio with Al content can be explained by the replacement of phosphorus atoms in the metaphosphate rings, through solid-solution formation as indicated by the change in lattice parameters. The phosphorus environment thereby changes from $Q_0^2$ to $Q_1^1$ which is consistent with the appearance of $^{31}P$ resonances at the low-frequency edge of band B for ceramics **2** and **3**. The $Q^1/Q^2$ ratio will also be influenced by ring opening of the cyclic metaphosphates and depolymerisation; a process suggested by Hartmann *et al.*[5] to be catalysed by aluminium. The $Na_5Ca_2Al(PO_4)_4$ structure proposed[22] as a component of ceramic **3** has aluminium tetrahedrally coordinated by four crystallographically distinct $Q_1^0$ $PO_4$ groups. The $^{31}P$ chemical shift for $Q_1^0$ species has not been reported, but almost certainly it will occur within the range covered by band B. Certainly the observation of a significant tetrahedral

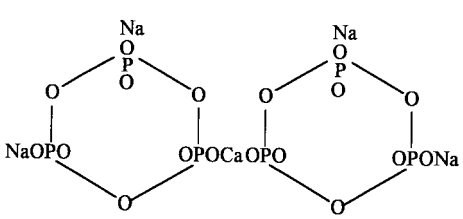


**Fig. 9** The suggested[34] structure for $Na_4Ca(PO_3)_6$

$^{27}Al$ signal from ceramic **3** (Table 3) is consistent with the presence of $Na_5Ca_2Al(PO_4)_4$.

On the basis of the NMR data alone the phases in the ceramics could include the distinct[35,36] crystal modifications of sodium metaphosphate, $(NaPO_3)_n$, or cyclic structures as in $Na_3P_3O_9$. From the isotropic chemical shifts it is possible[37] that these $Q^2$ units have sodium and/or calcium ions in the second coordination sphere of phosphorus although Fletcher *et al.*[7] reported $^{31}P$ $Q^2$ shifts from binary calcium phosphate glasses to somewhat lower frequency, in the region $\delta$ $-25$ to $-28$.

The appearance of band B is different for the three ceramics. The most salient feature (see Fig. 7) is the number of distinct chemical shifts, and this must be due to a complex mixture of phases wherein the $Q^1$ phosphorus atoms have different combinations of sodium and calcium and aluminium in their second coordination sphere. At the high-frequency edge of the band ($\delta$ *ca.* 0) $Q^1$ phosphorus influenced by sodium is expected, and with substitution by calcium, lower frequency $Q^1$ shifts occur. The presence of aluminium in the ceramics results in even lower frequency resonances, in the region $\delta$ $-11$ to $-16$, contributing to band B. This is in accord with the observations of Hartmann *et al.*[5] who assigned resonances in this region to $Q^1$ (Al, Ca, Na) species. For ceramic **2** these new aluminium-containing species are produced at the expense of species with resonances at the high-frequency edge of the band (sodium-dominated $Q^1$ units), and arise as described above by the conversions $Q_0^2 \rightarrow Q_1^1$ or $Q_0^1 \rightarrow Q_1^1$.

The patterns of the sharp resonances from ceramics **2** and **3** are similar, with the addition in ceramic **3** of a broad resonance (band C) centred at $\delta$ $-0.4$. The width of band C suggests it is due to an amorphous component in the sample. The isotropic chemical shift is consistent with calcium orthophosphate[31] $[Ca_3(PO_4)_2]$ or sodium pyrophosphate[30] $(Na_4P_2O_7)$. However the chemical shift anisotropy of band C is $\Delta\delta$ 141, which is close to that reported[37] ($\Delta\delta$ 127) for $Na_4P_2O_7$, and very different to that[38] for $Ca_3(PO_4)_2$ ($\Delta\delta$ 0). There is no corroborative evidence for the presence of $Na_4P_2O_7$ from the X-ray data since a low level of an amorphous phase would not give rise to identifiable features in the powder pattern.

With the higher level of aluminium in ceramic **3**, three new $^{31}P$ resonances appear (band D) at $\delta$ $-27.9$ (7.1%), $-28.7$ (3.5%) and $-30.6$ (0.7%). From consideration of the isotropic chemical shift alone these lowest frequency resonances could be due to one or more of the $AlPO_4$ polymorphs which are reported[29–31,33,38] to show resonances in the region $\delta$ $-24.5$ to $-29.5$. Another possibility for these resonances is $Q_1^2$ units[37] similar to those from $[Al(PO_3)_3]_n$ which has[32] its $^{31}P$ resonance at $\delta$ $-30$. The chemical shift tensor components for band D ($\delta_{ii}$ $-91$, $-35$ and 41) show some similarity with those for $[Al(PO_3)_3]_n$ ($\delta_{ii}$ $-120$, 15 and 15), with the chemical shift anisotropy being somewhat lower for band D ($\Delta\delta$ 104 *vs.* $\Delta\delta$ 135 for aluminium metaphosphate). However the values for the chemical shift tensor components and the chemical shift anisotropy for band D (see Table 4) are effective averages for the three component resonances. Therefore an interpretation of our data is that the major component of band D ($\delta$ $-27.9$) is a $Q_1^2$ resonance similar to that for aluminium metaphosphate, and either or both of the other two resonances are from $AlPO_4$ for which $\Delta\delta$ is expected[38] to be near zero. The presence of the $AlPO_4$ phase is also supported by the tetrahedral $^{27}Al$ resonance (see Table 3). The X-ray data do not provide evidence for or against the presence of these phases as such relatively low levels ($\leqslant 7\%$) would not be detected in the diffraction data.

## Conclusion

The solid-state $^{31}P$ spectra of the glass ceramics show a preponderance of $Q^2$ units, indicative of long-chain or cyclic

metaphosphates. The $^{23}Na$ spectral parameters are similar to those reported[12] for the cyclic trimetaphosphate $Na_3(PO_3)_3$, and the X-ray powder diffraction data shows the dominance of $Na_4Ca(PO_3)_6$ for which the structure is thought[34] to consist of bridged trimetaphosphate rings. The presence of the small ring structures, instead of the long-chain polyphosphates has relevance to the long-term solubility of the materials since the alkali-metal polyphosphates are highly insoluble.[39] Because the $Q^2$ environment dominates the materials, the $Q^1$ environment must therefore be largely due to pyrophosphate, $P_2O_7^{4-}$, and the various $Q^1$ resonances from the ceramics are due to the array of different pyrophosphates possible in the presence of the mixed cations. The broad, high-frequency band C in ceramic **3** is probably mostly due to amorphous $Na_4P_2O_7$ in the sample, in spite of the increased time employed for the ceramic formation (Table 1). The higher level of aluminium in this sample may result in less efficient crystallisation of the $Q^1$ phases through Al cross-linking of the phosphate species. The $^{27}Al$ spectra of samples **2** and **3** show that the aluminium is predominantly present with octahedral coordination, and at the higher concentration (5% in sample **3**) there is additionally four-coordinate aluminium. The X-ray powder pattern for ceramic **3** indicates the presence of $Na_5Ca_2Al(PO_4)_4$ for which the $Q_1^0$ $^{31}P$ resonances would fall within band B. The lowest frequency band D in the $^{31}P$ spectrum of ceramic **3** could be due to $Q_1^2$ phosphorus similar to that in aluminium metaphosphate, but we cannot exclude the possibility of contributions from $Q_4^0$ sites from one or more of the polymorphs of $AlPO_4$.

The $Q^1/Q^2$ ratio for both samples **2** and **3** shows a significant increase upon ceramic formation, which does not occur for sample **1**. Hartmann *et al.*[5] have made a similar observation for Na/Ca/Al/phosphate glasses and ceramics and have speculated that the aluminium in some way catalyses the depolymerisation of the metaphosphate during ceramic formation. It is noteworthy that the $Q^1/Q^2$ ratios for the glasses in this study did not vary significantly with $Al_2O_3$ content, and this effect certainly merits further study. Our observation that the $Q^1/Q^2$ ratio in the aluminium-free sample **1** is not significantly different between the glass and the ceramic raises the possibility of using the more detailed structural information from aluminium-free ceramics to model the phosphate structures in glasses.

We wish to thank the University of London Intercollegiate Research Service in Solid State NMR at University College for the provision of the MSL-300 NMR spectrometer, and Dr. P. J. Barrie, Dr. A. E. Aliev and Mr. D. Butler for measuring the one-dimensional spectra. We also thank the IRC in Biomedical Materials at QMW for use of a diffractometer and thermal analysis equipment. G. P. acknowledges the receipt of a studentship from the EPSRC, and K. F. received support from the EC ERASMUS programme.

## References

1 H. Aoki, *Science and Medical Applications of Hydroxyapatite*, Takayama Press Syste, Centre Co. Inc., Tokyo, JAAS, 1991.
2 K. Kawanabe, T. Yamamuro, T. Nakamura and S. Kotani, *Bioceramics*, ed. G. Heimke, Deutsche Keramische Geselleschaft, Köln, 1990, vol. 2, p. 121, and references therein.
3 W. Vogel and W. Höland, *Angew. Chem., Int. Ed. Engl.*, 1987, **26**, 527.
4 R. J. Kirkpatrick and R. K. Brow, *Solid State NMR*, 1995, **5**, 9.
5 P. Hartmann, J. Vogel and B. Schnabel, *J. Non-Cryst. Solids*, 1994, **176**, 157.
6 P. Hartmann, J. Vogel and C. Jäger, *Ber. Bunsenges. Phys. Chem.*, 1996, **100**, 1658.
7 J. P. Fletcher, R. J. Kirkpatrick, D. Howell and S. H. Rishbud, *J. Chem. Soc. Faraday Trans.*, 1993, **89**, 3297.
8 R. K. Brow, R. J. Kirkpatrick and G. L. Turner, *J. Non-Cryst. Solids*, 1990, **116**, 39.
9 C. Jäger, M. Feike, R. Born and H. W. Spiess, *J. Non-Cryst. Solids*, 1994, **180**, 91.
10 R. Born, M. Feike, C. Jäger and H. W. Spiess, *Z. Naturforsch. A*, 1995, **50**, 169.
11 R. K. Sato, R. J. Kirkpatrick and R. K. Brow, *J. Non-Cryst. Solids*, 1992, **143**, 257.
12 H. Koller, G. Engelhardt, A. P. M. Kentgens and J. Sauer, *J. Phys. Chem.*, 1994, **98**, 1544.
13 J. Burnie, PhD Thesis, University of Strathclyde, 1982.
14 L. Frydman and J. S. Harwood, *J. Am. Chem. Soc.*, 1995, **117**, 5367.
15 C. Fernandez and J. P. Amoureux, *Chem. Phys. Letts.*, 1995, **242**, 449.
16 C. Fernandez and J. P. Amoureux, *Solid State NMR*, 1996, **6**, 315.
17 J. P. Amoureux, C. Fernandez, L. Carpentier and E. Cochon, *Phys. Status Solidi A*, 1992, **132**, 461.
18 J. Herzfeld and A. E. Berger, *J. Chem. Phys.*, 1980, **73**, 6021.
19 G. E. Hawkes, K. D. Sales, L. Y. Lian and R. Gobetto, *Proc. R. Soc. London, Ser. A*, 1989, **424**, 93; G. E. Hawkes, K. D. Sales, S. Aime, R. Gobetto and L. Y. Lian, *Inorg. Chem.*, 1991, **30**, 1489.
20 U. Haeberlen, *High Resolution NMR in Solids—Selective Averaging*, Academic Press, New York, 1976, p. 9.
21 J-C. Grenier, C. Martin and A. Durif, *Bull. Soc. Fr. Mineral. Cristalogr.*, 1970, **93**, 52.
22 J. Alkemper, H. Paulus and H. Fuess, *Z. Kristallogr.*, 1994, **209**, 76.
23 H. M. Ondik, *Acta Crystallogr.*, 1965, **18**, 226.
24 R. K. Brow, R. J. Kirkpatrick and G. L. Turner, *J. Am. Ceram. Soc.*, 1993, **76**, 919.
25 D. Müller, G. Berger, I. Grunze, G. Ladwig, E. Hallas and U. Haubenreisser, *Phys. Chem. Glasses*, 1983, **24**, 37.
26 R. Dupree, I. Farnan, A. J. Forty, S. El-Mashri and L. Bottyan, *J. Phys.*, 1985, **46**, C8.
27 H. Haubenreisser, J. Vogel, W. Höland and W. Vogel, *Wiss. Ztschr. Friedrich-Schiller-Univ. Jena, Naturwiss. R.*, 1987, **36**, 763.
28 R. K. Brow, R. J. Kirkpatrick and G. L. Turner, *J. Am. Ceram. Soc.*, 1990, **73**, 2293.
29 G. L. Turner, K. A. Smith, R. J. Kirkpatrick and E. Oldfield, *J. Magn. Reson.*, 1986, **70**, 408.
30 A. K. Cheetham, N. J. Clayden, C. M. Dobson and R. J. B. Jakeman, *J. Chem. Soc., Chem. Commun.*, 1986, 195.
31 S. Prabhakar, K. J. Rao and C. N. Rao, *Chem. Phys. Lett.*, 1987, **139**, 96.
32 A. R. Grimmer and G. U. Wolf, *Eur. J. Solid State Inorg. Chem.*, 1991, **28**, 221.
33 D. Müller, E. Jahn, G. Ladwig and U. Haubenreisser, *Chem. Phys. Lett.*, 1984, **109**, 332.
34 E. J. Griffith, *Inorg. Chem.*, 1962, **1**, 962.
35 K. H. Jost, *Acta Crystallogr.*, 1961, **14**, 844.
36 K. H. Jost, *Acta Crystallogr.*, 1963, **16**, 640.
37 T. M. Duncan and D. C. Douglass, *Chem. Phys.*, 1984, **87**, 339.
38 I. L. Mudrakovskii, V. P. Shmachkova, N. S. Kotsarenko and V. M. Mastikhin, *J. Phys. Chem. Solids*, 1986, **47**, 335.
39 D. E. C. Corbridge, *The Structural Chemistry of Phosphorus*, Elsevier, Amsterdam, 1974, ch. 6.

*Paper* 6/08325K; *Received* 10*th December*, 1996